This article has been accepted for publication in a future issue of this journal, but has not been fully edited. Content may change prior to final publication. Citation information: DOI 10.1109/ACCESS.2022.3142168, IEEE Access

IEEE Access
Multidisciplinary ⋮ Rapid Review ⋮ Open Access Journal

Date of publication xxxx 00, 0000, date of current version xxxx 00, 0000.

*Digital Object Identifier 10.1109/ACCESS.2017.Doi Number*

# Characteristic Study of Solar Photovoltaic Array under Different Partial Shading Conditions

**Kais Abdulmawjood[1,2], Member, IEEE, Samer Alsadi[3,1], Senior Member, Shady S. Refaat[1], Senior Member, IEEE, Walid G. Morsi[2], Senior Member**

[1]Electrical and Computer Engineering Department, Texas A&M University at Qatar, Doha, Qatar
[2]Electrical Engineering Department, Ontario Tech University (UOIT), Oshawa, ON, Canada
[3]Electrical Engineering Department, Palestine Technical University-Kadoorie

Corresponding author: Kais AbdulMawjood (e-mail: kais.abdulmawjood@qatar.tamu.edu).

Open Access funding provided by the Qatar National Library.

**ABSTRACT** Photovoltaic (PV) systems are frequently exposed to partial or complete shading phenomena. Partial shading has a profound impact on the performance of solar power generation. The operational performance of PV arrays under partial shading shows multiple maximum power point peaks, therefore it is challenging to identify the actual maximum power point. This paper investigates the impact of partial shading location on the output power of solar photovoltaic arrays with various configurations. Multiple photovoltaic strings, in both parallel and series configurations, are considered. Different random shading patterns are considered and analyzed to determine which configuration has higher maximum power point. The sensitivity of the partial shading can change according to the partial shading types, shading pattern, and the configuration used to connect all PV modules. Moreover, the study also investigates the output of the PV array with shading two random models, two consecutive models, and three random and consecutive modules. Experimental results validate the analysis and demonstrate the effect of various partial shading on the efficiency and performance of the PV system.

**INDEX TERMS** Photovoltaic system, partial shading, P-V characteristics, configuration, shading patterns.

## I. INTRODUCTION

PV modules are combined in series-parallel configurations to obtain a desired output voltage and current levels. The partial of the complete shading of PV modules is a common incident and it results in reducing the output power of the PV system significantly. Partial shading broadly falls into two categories; static and dynamic shading. In the static shading type, a particular shadow stays fixed on the PV array for an extended period of time such as dust or dirt accumulation or bird droppings adhered to the PV surface. Meanwhile, dynamic shading type occurs due to covering part of the PV array with tree leaves, shade of a neighboring construction, passing clouds, or smoke.

In recent years, there is a growing concern about the most effective PV configuration to generate the maximum power by reducing the mismatching loss under different shading conditions. Photovoltaic cells under shading conditions produce less photon current. The generated photon current depends on the PV cell area and the cells irradiation [1], which consequently results in mismatching the current generated by the nearby fully illuminated cells. Under such conditions, the shaded cells may get reverse biased and act as load, which leads to power loss [2]. Hence, hot-spot heating occurs, and the system can be irreversibly damaged if it is not protected appropriately. Many topologies have been proposed to investigate various PV array configurations under different patterns such as series (S), series-parallel (SP), total cross-tied (TCT), bridge link (BL), honeycomb (HC) and complementary metal oxide semiconductor (CMOS)-embedded for PV panels [2].

However, these topologies lack many aspects in terms of the mechanism to isolate the PV cells and effectively deal with the shading conditions. The bypass diodes are commonly used in parallel with a series-connected cells or a complete module to minimize the effect of the partial shading. These diodes create further losses due to their ON-state resistance [3]. Moreover, the partial shading causes multiple power peaks in PV output power and results in misleading the maximum power point

This article has been accepted for publication in a future issue of this journal, but has not been fully edited. Content may change prior to final publication. Citation information: DOI 10.1109/ACCESS.2022.3142168, IEEE Access



tracker (MPPT), which can be added to the losses [3-4]. Therefore, more comparative investigations are required to better understand the effectiveness of reconfiguring PV modules. This will help scientists, designers, and manufacturers to improve the partial shading mitigation topologies for PV arrays.

In this paper, the authors assess the power performance of serial-parallel topology PV array power when partially or completely shading models are located in different locations of a solar PV array.

This research work aims to investigate the effectiveness of various reconfigurations on the characteristics of PV arrays under partially shaded conditions. The influence of shading multiple modules on the low voltage peak is discussed considering different shading patterns and heaviness applied to unsymmetrical size of array systems. Furthermore, a mathematical formula is presented to calculate the low voltage power peak that is applicable for photovoltaic array systems with different number of shading modules. The formula was evaluated and verified with different photovoltaic array configurations constructed from models of the same manufacturing specifications.

This paper is organized as follows. Section II presents the mathematical modelling of the solar cell. Section III provides an in-depth discussion on PV array configuration. Section IV describes the simulation results of the PV arrays under partial shading. Section V presents the experimental validation and the operational performance analysis. Conclusion is given in section VI.

## II. MATHEMATICAL MODELLING OF SOLAR CELL

Photovoltaic systems can be sorted based on the desired power generation level, or based on the system configuration, or the type of the connection to the grid. A typical PV system comprises of four major parts: the PV arrays, power conditioner [14], storage system, and the PV inverter. The system is connected to the utility grid with or without a local load.

Solar cells are combined in series to construct a string, and strings are connected in parallel to construct a PV module. To assemble a PV array, modules are combined in series and/or in parallel to match the electric power demand. There are common models for a PV cell: ideal single diode model, simplified single diode model, improved single diode model, and two model diode model [15]. Figure 1 shows the single-diode equivalent model of a solar cell. The model corresponding equations are as follows [16]:

$$I_L = I_{ph} - I_d - I_{sh} \quad (1)$$

$$I_d = I_o\left[e^{\frac{V+R_S I_L}{nV_t}} - 1\right] \quad (2)$$

$$\mathrm{I_{sh}} = \frac{\mathrm{V+ I_L R_S}}{\mathrm{R_{sh}}} \quad (3)$$

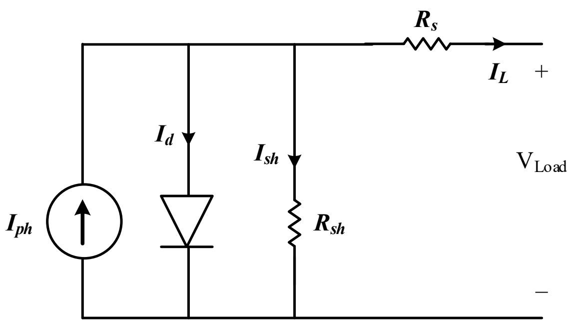


**FIGURE 1.** **Equivalent circuit for single-diode model**

**TABLE I**
**MODULE ELECTRIC CHARACTERISTICS**

| Parameter | Value |
|---|---|
| Maximum Power (W) | 250 |
| Current at mpp (A) | 8.07 |
| Voltage at mpp(V) | 30.96 |
| Short-circuit Current (A) | 8.62 |
| Open-circuit voltage (V) | 37.92 |
| Cells per module | 60 |
| Light Generated Current (A) | 8.6307 |
| Diode saturation current | 1.4176e-10 |
| Diode ideality factor | 0.99132 |
| Shunt resistance $R_{sh}$ (ohms) | 82.1161 |
| Series resistance $R_s$ (ohms) | 0.098625 |
| Temperature coefficient of $V_{oc}$(%/deg.C) | -0.33969 |
| Temperature coefficient of $I_{sc}$(%/deg.C) | 0.063701 |

$$I_L = I_{ph} - I_o\left[e^{\frac{V+R_S I_L}{nV_t}} - 1\right] - \frac{V+R_S I_L}{R_{sh}} \quad (4)$$

where $I_o$ is the diode reverse saturated current, $V_t$ is diode thermal voltage, K is Boltzmann constant, $q$ is electron charge, and $n$ is the quality factor of the diode, which is derived from the slope of the dark-IV and the light-IV curves [18] and its value is between 1 and 2. The models for PV module have been designed and implemented using the MATLAB/Simulink environment based on the Shockley diode equation mentioned above. The simulation results for a uniform and non-uniform irradiance show excellent correspondence to the power-voltage (P-V) characteristic of the PV array [17]. A one diode model has been utilized in this work and the proposed model was connected in series and parallel to simulate PV arrays with different combinations.

## III. PV Array Configuration

The proposed PV module comprises 60 solar cells arranged into three assemblies connected in parallel, where each assembly contains 20 cells in series. Table I lists the electric characteristics for the developed module. The bypass diodes were added in parallel to each branch. The behavior characteristics of any PV array with bypass diodes differ from those without bypass diodes as these diodes introduce multiple peaks in addition to changing some local or global maximum power points values or locations [19]. There are many configuration topologies to construct and model PV arrays that

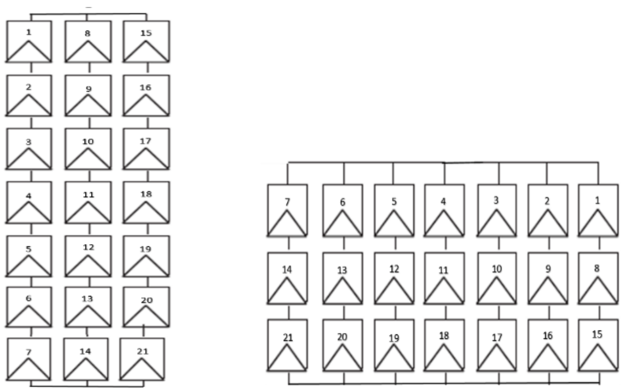


(a) (b)

**FIGURE 2. Array Configurations**

have been discussed in [19]-[21]. Among these configurations, the serial-parallel (SP) is widely used in modeling to reduce the calculation time without losing accuracy for different applications like estimation of energy production for a PV array in its lifetime. The modules in the SP configurations are first connected in series to obtain the required voltage, and then connected in parallel to generate the desired power level.

The proposed PV array consists of 21 panels to assemble a system with maximum power of 5.25 kW during no shade uniform irradiance condition. Two different serial-parallel configurations were considered in this work. The first configuration consists of three parallel-connected strings, and each string is constructed from seven modules series-connected as shown in Figure 2-(a). The PV array generates output voltage of 265 volt in normal operation. The second proposed configuration is constructed from seven parallel-connected strings, where each string is limited to three series-connected modules as shown in Figure 2-(b). The PV array is designed to generate 113 volts at no load. The work presented in this study aims to study the effect of shading uniform and non-uniformed irradiance and locations on the array's output power by considering different shading combinations of the 21 modules.

## IV. Simulation Results

This section describes modeling procedures for simulating the V-I and P-V characteristics of PV array system under partial shading. It is important to understand the effect of the shading pattern and its level by considering all possible locations for a certain number of shaded modules under different percentage of illuminance. This procedure consists of defining two different array configurations as shown in Figure 2, where both configurations consist of 21 PV modules. In the first configuration the PV modules are arranged into three parallel-connected assemblies each having seven series-connected modules. On the other hand, the second configuration consists of seven parallel-connected assemblies, each having three series-connected modules.

TABLE II
SHADING PATTERNS OF THE ARRAY USED IN CONFIGURATION 1

| Shading Pattern | Total Shaded Modules | Number of shaded modules (NS) | | |
|---|---|---|---|---|
| | | Assembly 1 | Assembly 2 | Assembly 3 |
| P1* | 2 | 2 | 0 | 0 |
| P2 | 2 | 1 | 1 | 0 |
| P3* | 3 | 3 | 0 | 0 |
| P4 | 3 | 2 | 1 | 0 |
| P5 | 3 | 1 | 1 | 1 |
| P6* | 4 | 4 | 0 | 0 |
| P7 | 4 | 3 | 1 | 0 |
| P8 | 4 | 2 | 2 | 0 |
| P9 | 4 | 2 | 1 | 1 |

* *Adjacent and random distributed modules were considered*

### A. Configuration 1

Considering the PV array system shown in Figure 2-(a), it is desired to obtain the *I-V* and *P-V* characteristics for this PV array with various shading patterns. First, a considered uniform shading is subjected to all PV modules at five different levels of irradiance. Figure 3-(b) shows the resulted *P-V* output characteristics of the setup during five irradiance levels. The selected modules in series assemblies were subjected to shading and the *I-V* and *P-V* characteristics of the PV array are displayed. The shaded patterns set used in testing this configuration are listed in Table II. In the first shading pattern *P1*, two modules were selected randomly in the same series assembly. The two modules were shaded by applying five different levels of irradiance starting from fully shaded modules to only 20% shading irradiance. Figure 4(a) shows the *I-V* and *P-V* characteristics respectively for the entire PV array while applying different shading levels. Instead of selecting random modules, the aforementioned test was reconducted using two series adjacent modules. The measured output characteristics found are similar to the *I-V* and *P-V* characteristics results while shading two random modules in

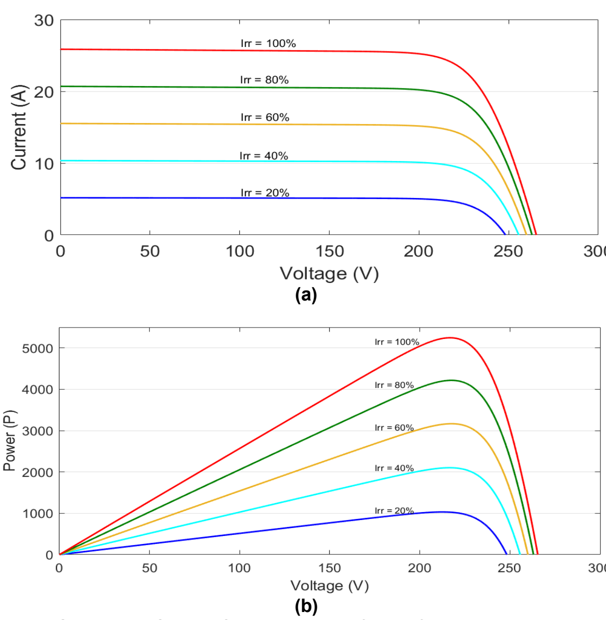


**FIGURE 3. Output Characteristics for uniform shading test**

IEEE Access
Multidisciplinary ⋮ Rapid Review ⋮ Open Access Journal

the same series assembly but not adjacent. Considering the *P-V* characteristics shown in Figure 4-(a), the higher voltage peaks of the P-V characteristics are higher than the lower voltage peak when module irradiance is more than 20%. The second shading pattern *P2* considers again the shading of only two modules in the PV array but in this test the modules are selected randomly on two separate assemblies. Figure 4-(b) illustrates the *I-V* and *P-V* characteristics of the PV array with two shaded modules on separate assemblies. The *P-V* characteristics shows that higher voltage peaks of the *P-V* characteristics are higher than the lower voltage peak only when module irradiance is above 75%. The higher voltage peak increases as the module irradiance increases.

Another set of simulation for shading patterns: *P3*, *P4* and *P5* mentioned in Table II are conducted considering three shaded modules. In the first simulation test, the three modules are selected randomly in the same series assembly and the *V-I* and *P-V* characteristics of PV array are shown in Figure 5-(a) respectively. The characteristics of the PV array become the same when the shaded modules are series adjacent and located in the same assembly. The *P-V* characteristics of this shaded setup show that the higher voltage peaks of the P-V characteristics are higher than the lower voltage peak for all considered irradiance levels. In the second simulation, three shaded modules located on two assemblies are considered and the array output *V-I* and *P-V* characteristics are displayed in Figure 5-(b) correspondingly. The *P-V* characteristics display multiple local peaks (LPs) and one global peak (GP). The global peak is the highest among all peak points. The third simulation test was conducted while locating one shaded module per assembly and the resulted output *V-I* and *P-V* characteristics are shown Figure 5-(c). The *P-V* characteristics illustrates that higher voltage peaks of the *P-V* characteristics are higher than the lower voltage peak only when module irradiance is above 75% and the output peak increases as the module irradiance increases.

Finally, similar simulation trials were conducted using four shaded modules. The shaded modules were located on one, two and three assemblies as mentioned in Table II. As mentioned in P6 shading configuration, the four shaded modules were selected randomly and then four series adjacent modules were considered in the simulation. The *V-I* and *P-V* characteristics of PV array are shown in Figure 6-(a) respectively. The resulted *P-V* characteristics are the same when the shaded modules were randomly or adjacently located in the same assembly. The *P-V* characteristics of this shaded setup shows that the higher voltage peaks of the P-V characteristics are higher than the lower voltage peak for all considered irradiance levels.

The simulations were conducted by shading four panels located on two assemblies as mentioned in in shading patterns P6 P7, P8 and P9. The resulted output V-I and P-V characteristics using four shaded modules for the aforementioned patterns are shown in Figure 6.

In the first simulation test, the three modules ware selected randomly in the same series assembly and the *V-I* and *P-V* characteristics of PV array are shown in Figure 6-(a) respectively. The characteristics of the PV array become the same when the shaded modules are series adjacent at the same assembly. The *P-V* characteristics of this shaded setup shows that the higher voltage peaks of the P-V characteristics are higher than the lower voltage peak for all considered irradiance levels.

Figure 6-(b) shows the *V-I* and *P-V* characteristics when three modules are shaded in one assembly and only one module shaded on another assembly. The third assembly has no shaded module in this test. The *P-V* characteristics of this setup shows multiple peaks and higher voltage peaks of the *P-V* characteristics are higher than the global peak only when module irradiance is above 35%.

Next, two modules were randomly shaded on each of two assemblies while no shading applied on the third assembly and the resulted *V-I* and *P-V* characteristics are shown in Figure 6-(c). The *P-V* characteristics shows that higher voltage peaks are higher than the lower voltage peak (GP) only when module irradiance is above 50%.

### *B. Configuration 2*

The PV array system shown in Figure 3(b) was also simulated by applying the same shading patterns listed in Table II in addition to one more pattern case in which the shading was applied to four randomly selected modules distributed on four different assemblies. The *P-V* curves of the PV array were investigated while changing the irradiance over five levels. Figure 7 shows the resulting *V-I* and *P-V* characteristics while considering four shaded modules and each of these shaded modules is located randomly on a single assembly. The *P-V* characteristics illustrates that when module irradiance is 20% and above, higher voltage peaks are higher than the lower voltage peak and the output peak increases as the module irradiance increases.

### *C. P-V* characteristic *curves*

It is obvious that PV modules connected in series will carry the same current, but the voltage across each module could be different depending on the applied irradiance to that module. Thus, the resulting output voltage for a series assembly is obtained by adding-up modules voltages while the assembly current is limited to the shaded module current. It should also be mentioned that when connecting a group of series assemblies in parallel, a common voltage is considered for the group output voltage while the group current is a result of adding-up assemblies' currents.

To prove the behavior of the output characteristic, the PV array system shown in Figure 11 is considered. The setup has three shaded PV modules located on the same string. Each string with unshaded photovoltaic modules can generate 8.07A while the string with shaded modules generates 4.52A at 60% shading irradiance.

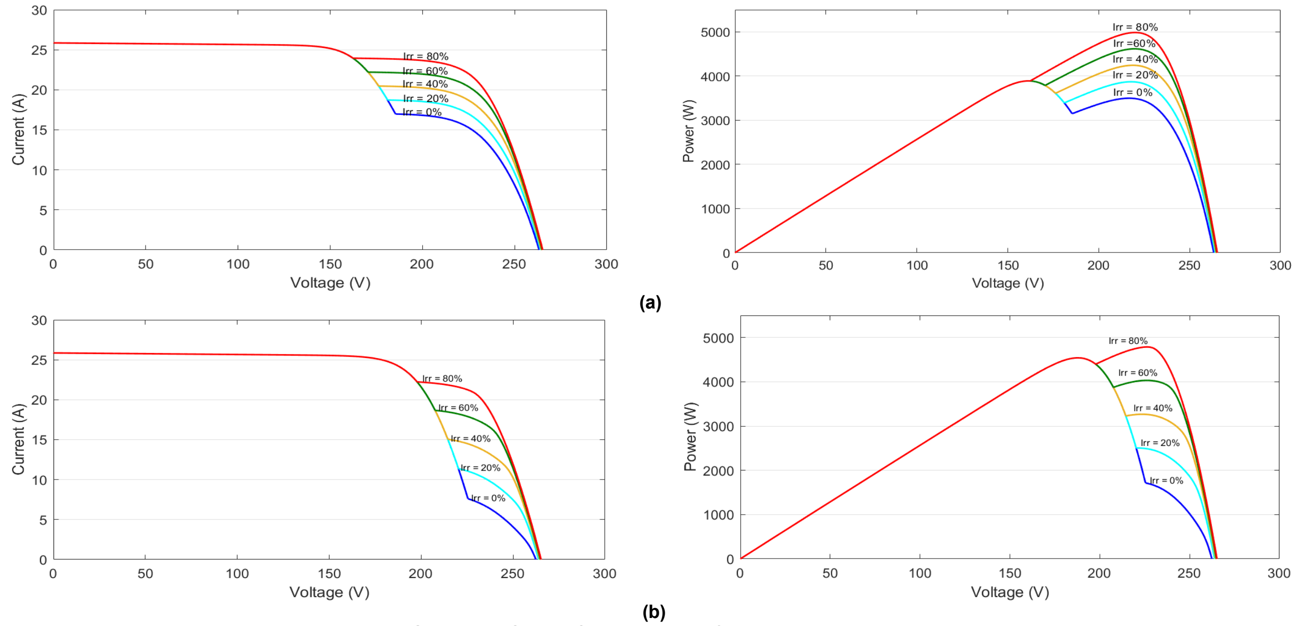


**FIGURE 4. Output Characteristics for 2 shaded modules**
**(a) Located in same string, (b) Located in two different strings**

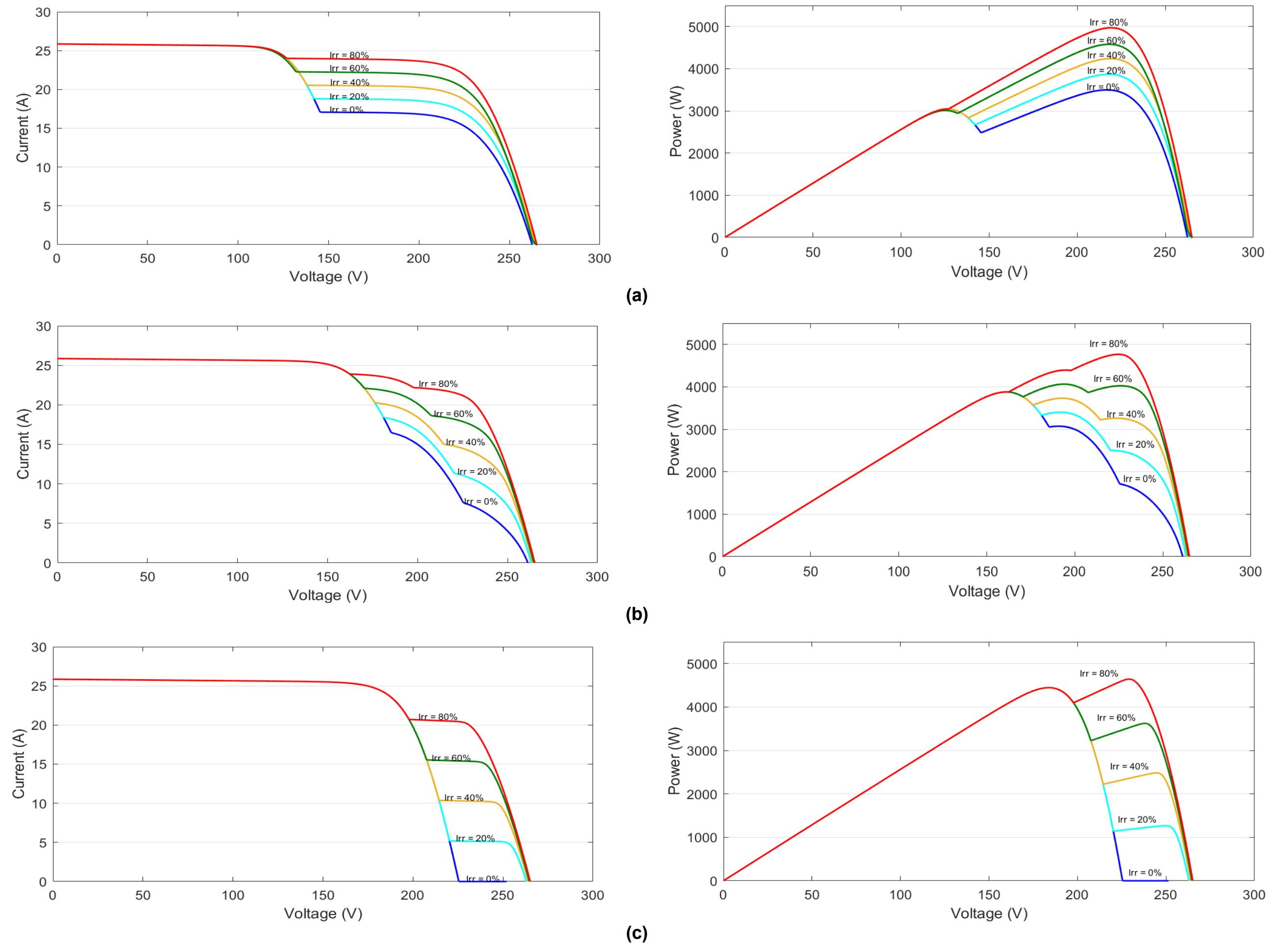


**FIGURE 5. Output Characteristics for 3 shaded modules**
**(a) Located on a single string, (b) Located on two string, (c) Located in three strings**

IEEE Access
Multidisciplinary ⋮ Rapid Review ⋮ Open Access Journal

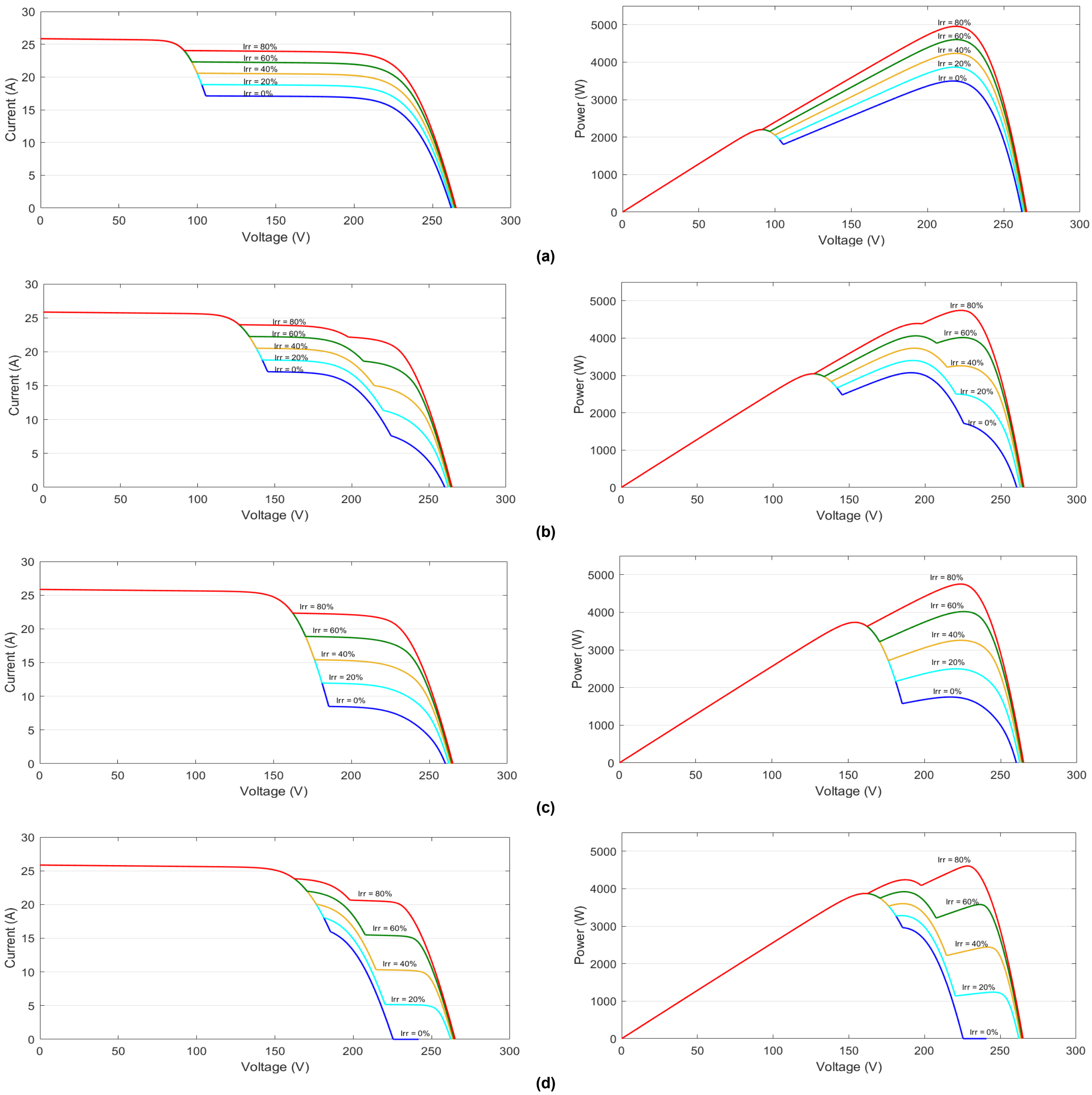


**FIGURE 6. Output Characteristics for 4 shaded modules**
**(a) 4 shaded panels located on same string, (b) 3 and 1 shaded panels located on two strings,**
**(c) 2 and 2 shaded panels located on two strings, (d) 2, 1 and 1 shaded panels located on three strings respectively**

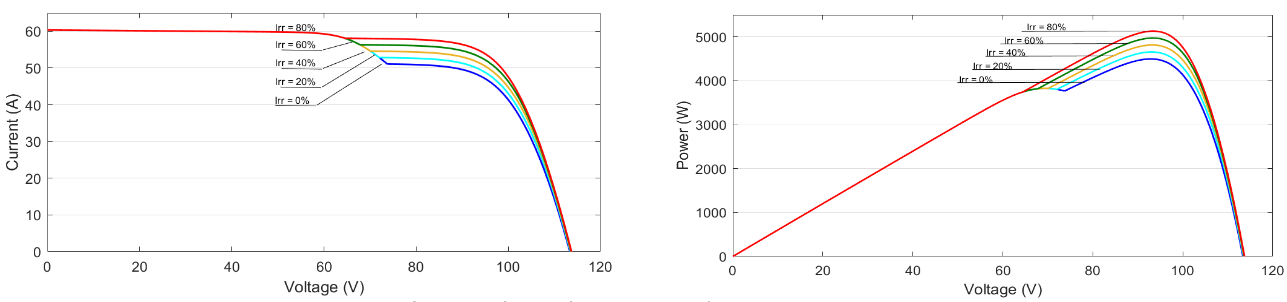


**FIGURE 7. Output Characteristics for 4 shaded modules**

IEEE Access
Multidisciplinary ⋮ Rapid Review ⋮ Open Access Journal

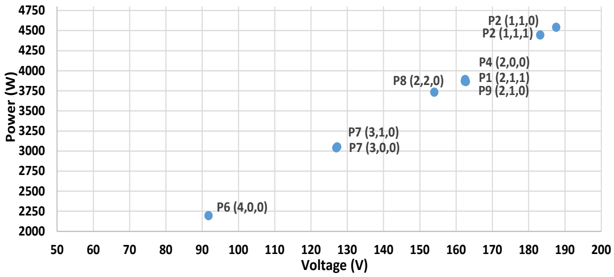


FIGURE 8. Global peaks of shaded patterns for first configuration

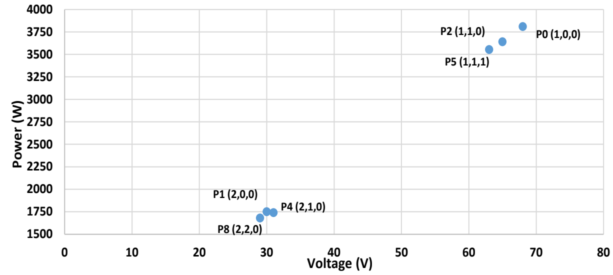


FIGURE 9. Global Peaks for shaded patterns for second configuration

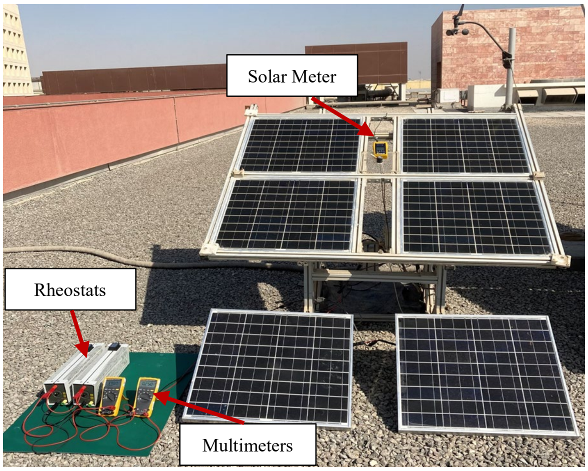


FIGURE 10. PV System of 6 modules

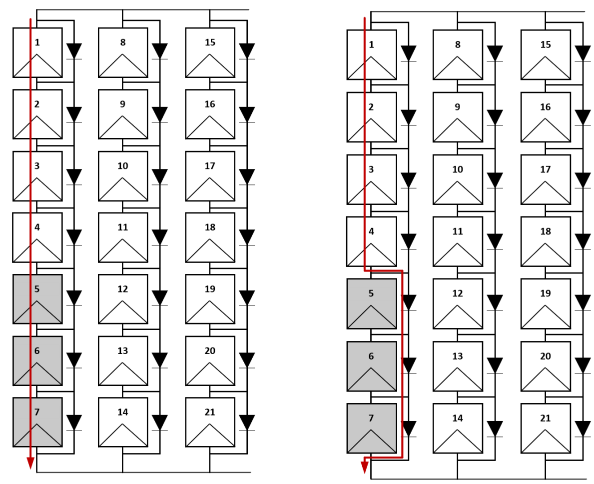

(a) Load current less than 4.52A (b) Load current more than 4.52A

FIGURE 11. PV system while shading

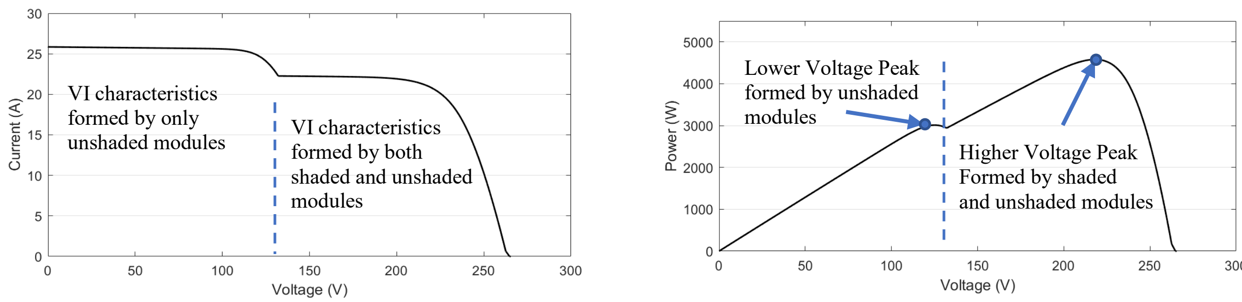


(a) (b)

FIGURE 12. PV system while shading
(a) *V-I* Characteristics, (b) *P-V* Characteristics

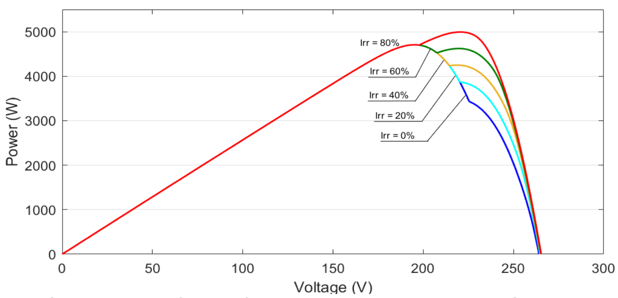


FIGURE 13. *P-V* Output Characteristics while shading Single Module

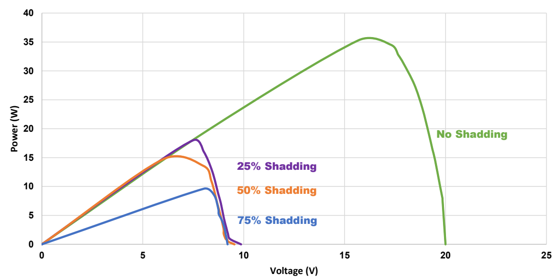


FIGURE 14. P-V Output Characteristics of a Single Module

IEEE Access
Multidisciplinary ⋮ Rapid Review ⋮ Open Access Journal

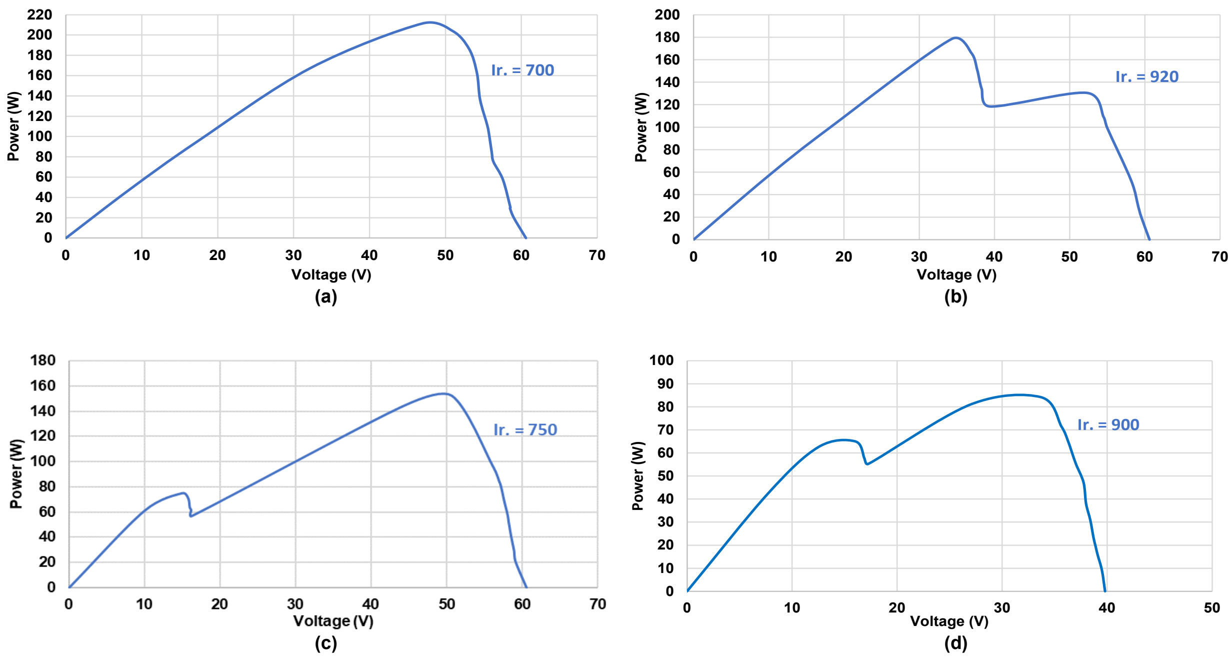


**FIGURE 15.** ***P-V*** **Characteristics for experimental setup**
**(a) No shading, (b) Single Module shaded, (c) Two In-Series Shaded Modules, (d) Three Shaded Modules Located at Two Assemblies**

When the load current drawn from the string with shaded modules is less than 4.52A, shaded modules are not overridden and the current generated flows through shaded modules as illustrated in Figure 11-(a). Consequently, the high-voltage side of the *V-I* characteristics shown in Figure 12-(a) are formed by both shaded and unshaded photovoltaic modules. Hence, the *V-I* characteristics are influenced by the change of irradiance level.

When the load current drawn from the string with shaded modules is more than 4.52A, shaded modules are overridden by the bypass diodes. Hence, the generated current by unshaded string modules is directed to the load without flowing through shaded modules as shown in Figure 11-(b). Therefore, the low-voltage side of *V-I* characteristics are formed by only the unshaded photovoltaic modules as indicated in Figure 12-(a). Accordingly, variation in irradiance of shaded modules doesn't affect the IV characterizes at currents above 4.52A.

Figure 12-(b) illustrate the *P-V* characteristics for the configuration of the PV array system under investigation. The characteristics show that the higher voltage is formed by the *V-I* characteristics below 4.52A, while the lower voltage is formed by the *V-I* characteristics above 4.52A. Hence, this validates that the higher voltage peaks of *P-V* characteristics are formed by the string shaded and unshaded photovoltaic modules. Therefore, the higher voltage peaks are subject to the irradiance of shaded photovoltaic modules. Furthermore, lower voltage peaks are formed by unshaded photovoltaic modules only and thus are unsusceptible to irradiance variation.

Considering the shading patterns P1 to P9 listed in Table II, the resulted *P-V* characteristics illustrate a single global peak (GP) for each shading pattern. Figure 8 shows the global peak distribution for the shading patterns under investigation and each point is labeled according to the pattern and the number of shaded modules per assembly.

The equation below determines the global peak (GP), which is obtained from Figure 8 using linear regression.

$$PG \approx -5495 \times \frac{Maximum\ number\ of\ shaded\ modules\ per\ assembly}{Number\ of\ modules\ per\ assembly} + 5450 \quad (5)$$

To validate equation (5), one module randomly selected is exposed to five different levels of irradiance starting from full shading to 20% shading level. Figure 13 shows the *P-V* characteristics for the five irradiance levels with global peak equal to 4680W. The global point obtained from the simulation results resemble the global point determined using equation (5). Moreover, Figure 9 illustrate the global peaks distribution resulted from the P-V characteristics of the PV array configuration shown in Figure 2-(b). Likewise, the global points resulted from simulations match the global point calculated using equation (5). Therefore, equation (5) is valid for the system under investigation for different shading patterns and sizes of photovoltaic string. It should be mention that the constants mentioned in equation 5 are function of the *P-V* characteristics.

Figures 4, 5, 6 and 7 reveal that multiple peaks existence that is equal to the number of different shading patterns of assemblies forming the array. Furthermore, it is seen from the *P-V* characteristics shown in Figure 5(c) and 7 that the common and local peaks appear when the assemblies have

IEEE Access
Multidisciplinary ⋮ Rapid Review ⋮ Open Access Journal

the same shading pattern. It is also observed from the resulted *P-V* characteristics at various irradiance levels that the first peak is common (GP) while the subsequent peaks (LP) are shifted more towards voltage axis as irradiance decreases.

In addition, the simulation results of the two configurations of the PV arrays show that it is preferred to increase the number of series assemblies connected in parallel since this would increase the maximum power obtained under the non-uniform irradiances. In general, it has been observed from the characteristic curves that the nature of curve including the number and magnitude of peaks depends on the array configuration, the irradiance level and the shading pattern.

## V. Experimental Validation

Two sets of experiments were conducted to investigate the impacts of partial shading on a PV array. The results obtained from the simulation are verified using a 324W experimental setup. The experimental setup of solar PV is shown in Figure 10. The setup consists of six Polycrystalline silicon (p Si) solar photovoltaic modules each of 54W, 12V manufactured by Kyocera (model KC50T). Table III lists the detailed specifications of the PV modules that are used at 1000Wm$^{-2}$ irradiance and 25°C cell temperature. The six modules are used to create a PV array consisting of two assemblies, each comprising of three modules connected in series. Two different sets of experiments were conducted. The first set of experiments were conducted by varying the shading area of a single PV module surface to investigate the shading effect on the PV module performance. A vertical shaded area was considered in this experiment using multiple layers of dark vinyl polyester fabric. The module was shaded by 25%, 50% and 75% while the irradiance level was 950W/m$^2$ at 29°C ambient temperature. Figure 14 illustrates the effect of partial shading on module output power while applying different shading ratios. The maximum output power dropped from 35.25W at no shading to 18W, 14.7W and 9.6W at shading 25%, 50% and 75% of the module surface respectively. It is found that the power dropped by 45.8%, 58.3% and 72.6% as the shading is increased by 25%, 50%, and 75%. Also, both the open circuit voltage ($V_{oc}$) and the short circuit current ($I_{sc}$) are decreased significantly with increasing shading area to 75% of module surface. The solar module power output is affected adversely by the shading area
and, as a result, the module efficiency is inversely proportional to the shading ratio. Another set of experiments were conducted by applying different shading patterns on the system's six modules to verify the previous simulation results. The patterns applied are shading one module, two in-series modules, and three modules located at two assemblies. Figure 15 shows the *P-V* output characteristics of the experimental setup without shading and with applying the aforementioned shading patterns. Figure 12-(a) shows the *P-V* output characteristics of the experimental setup at irradiance of 700Wm$^{-2}$. The maximum generated power is 211.5W at 47V output voltage. The *P-V* output characteristics while shading one module is shown in Figure 12-(b). Similar to the simulation results, the *P-V* characteristics show multiple peaks in this test and lower voltage peak of the *P-V* characteristics is higher when the irradiance is 920Wm$^{-2}$. However, the lower voltage peak of the *P-V* characteristics becomes lower than the high voltage peak while shading two modules in-series at irradiance of 750Wm$^{-2}$ as shown in Figure 12-(c). In the last experiment, three modules located on two assemblies are shaded, and Figure 12-(d) shows the output *P-V* characteristics at 900 Wm$^{-2}$. Again, the characteristics show two power output peaks similar to the previous experiment in Figure 12-(c). Also, the *P-V* characteristics demonstrate that the setup output power and the open-circuit voltage Voc are reduced with increasing the number of shading panels.

TABLE III:
KYOCERA MODEL KC50T POLYCRYSTALLINE SILICON SOLAR PHOTOVOLTAIC ELECTRICAL SPECIFICATIONS

| Electrical Data | |
|---|---|
| $P_{max}$ | 54W |
| $V_{max}$ | 17.4V |
| $I_{max}$ | 3.11A |
| $V_{oc}$ | 21.7V |
| $I_{sc}$ | 3.31A |
| Mass | 5.0 Kg |

*Note: The electrical specifications are under test of Irradiance of 1000Wm-2 and Cell Temperature of 25°C*

## VI. Conclusion

Photovoltaic array systems are highly influenced by shading. Complete or partial shading of a PV array drastically reduces the array power output. The reduction of the output power depends on the employed array configuration, the shading layout and the shading intensity. This paper presents the impact of different shading patterns on the P-V characteristics through performing a set of simulations with different array configurations. The shading PV arrays result in multiple local peaks and a global peak on the output P-V characteristics. The number of local peaks depends on the array configuration and the shading pattern. The obtained results also demonstrate that global peak can be reduced drastically when shaded modules are located on the same assembly. Furthermore, the value of the global peak is higher than the local peaks when the shaded modules are evenly distributed on different assemblies.

The proposed mathematical relationship to determine the low voltage power peak that is applicable for photovoltaic array systems with different number of shading modules. This relationship will help in anticipating shading modules that heavily impacts the power generated by the array. The formula was evaluated and verified with different photovoltaic array configurations constructed from models of the same manufacturing specifications. Furthermore, to corroborate the simulation data, experimental tests were conducted and the results showed strong similarity with the simulation.

## REFERENCES

[1] A. Yadav, V. Mukherjee, "Conventional and advanced PV array configurations to extract maximum power under partial shading conditions: A review", Renewable Energy, Vol. 178, pp. 977-1005, 2021.
[2] S. Bhattacharjee, A. Barbhuiya, et al., "An approach to enhance the efficiency of the solar PV panel in partial shading condition: A Review", AJEEE, vol. 2, Issue 1, February 2018.
[3] M. El-Dein, M. Kazerani, M. M. A. Salama, "Optimal Photovoltaic Array Configuration to Reduce Partial Shading Losses", IEEE Trans. on Sustainable Energy, Vol. 4, No. 1, pp. 145-153, 2013.
[4] R. Mahto, D. Sharma, D. Xavier and R. Raghavan, "Improving performance of photovoltaic panel by reconfigurability in partial shading condition", Journal of Photonics for Energy, Vol. 10(4), December 2020.
[5] A. C. Souza, F. C. Melo, T. L. Oliveira and C. E. Tavares, "Performance Analysis of the Computational Implementation of a Simplified PV Model and MPPT Algorithm", IEEE AL Transactions, vol. 14, no. 2, February 2016.
[6] S. Denga, Z. Zhang, Chenhui Jua, J. Donga, Z. Xiaa, X. Yana, T. Xua and G. Xinga, "Research on hot spot risk for high-efficiency solar module," Energy Procedia 130, pp. 77–86, 2017.
[7] S. Hamdi, D. Saigaa and M. Drif, "Modeling and simulation of photovoltaic array with different interconnection configurations under partial shading conditions for fill factor evaluation," International Renewable and Sustainable Energy Conference (IRSEC), 2014.
[8] R. Vieira, F. de Araújo, M. Dhimish, and. Guerra et al., "A Comprehensive Review on Bypass Diode Application on Photovoltaic Modules," Energies 13; 2472, 2020.
[9] B. Nadia, M. Ahmed, B. Nadia, Z. Nora, "Analysis of Solar Photovoltaic Array Interconnection Schemes Working Under Partial Shading Conditions," International Conference on Sustainable Renewable Energy Systems and Applications (ICSRESA), December 2019.
[10] A. Humada, F. Samsuri, M. Hojabria, et al., "Modeling of photovoltaic solar array under different levels of partial shadow conditions," International Power Electronics and Motion Control Conference and Exposition, Turkey, September 2014.
[11] YANG Yi, JI Sheng-lan, GU Hai-qin, C. Juan, "Simulation Study on Characteristics of Photovoltaic Array Under Partial Shading," Proceedings of the 33rd Chinese Control Conference, China, July 2014.
[12] S. Buragohain, S. Mahapatra, N. Sarmah, and S. Kumar, "Shading and Mismatch effect on the Performance of PV Module," International Conference on Advances in Energy Research (ICAER), Bombay, 2015.
[13] M. Premkumar, U. Subramaniam, Thanikanti S. Babu, R. M. Elavarasan, and L. Mihet-Popa, "Evaluation of Mathematical Model to Characterize the Performance of Conventional and Hybrid PV Array Topologies under Static and Dynamic Shading Patterns," Energies 2020, 13(12) - 3216, 2020.
[14] Singh, G. K., 2013, "Solar power generation by PV (photovoltaic) technology: A review", in Energy vol. 53, pp. 1-13, 2013.
[15] S. Bal, A. Anurag and B. C. Babu, "Comparative analysis of mathematical modeling of Photo-Voltaic (PV) array," in Proc. 2012 Annual IEEE India Conf. (INDICON), Kochi, pp.269-274, 2012
[16] Masmoudi F., Salem, F. B., Derbel, N., "Single and double diode models for conventional mono-crystalline solar cell with extraction of internal parameters", in IEEE 13th International Multi-Conference on Systems, Signals & Devices (SSD), pp. 720-728, 2016.
[17] K. Ding, X. Bian, H. Liu, and T. Peng, "A MATLAB-Simulink-Based PV Module Model and Its Application under Conditions of Nonuniform Irradiance", IEEE Trans. on Energy Conversion, VOL. 27, NO. 4, 2012.
[18] T. Nakamura, M. Imaizumi, Shin-ichiro Sato, and Takeshi Ohshima, "Change in I -V Characteristics of Subcells in a Multi-junction Solar Cell due to Radiation Irradiation", IEEE Photovoltaic Specialists Conference, Austin, TX, October 2012.
[19] H. Ziar; S. Mansourpour; E. Afjei; and M. Kazemi, "Bypass diode characteristic effect on the behavior of solar PV array at shadow condition", 3rd Power Electronics and Drive Systems Technology (PEDSTC), 2012.
[20] P. Satpathy, S. Jena, B. Jena, and S. Sharma, "Comparative Study of Interconnection Schemes of Modules in Solar PV Array Network," International Conference on circuits Power and Computing Technologies [ICCPCT], Kollam, India, 2017.
[21] R. Shaw, P. Walde and A. Ghosh, "Review and Analysis of photovoltaic arrays with different configuration system in partial shadowing condition," International Journal of Advanced Science and Technology, Vol. 29, no. 9s, 2020.
[22] J. C. Teo, Rodney H. G. Tan, and et al, "Impact of Partial Shading on the P-V Characteristics and the Maximum Power of a Photovoltaic String", Journal of Energies, 2018.
[23] J. D. Bastidas-Rodr´ıguez, D. Gonzalez, and C. A. Ramos-Paja "Model of Series-Parallel Photovoltaic Arrays Designed for Parallel Computing", 14th International Conference on Synthesis, Modeling, Analysis and Simulation Methods and Applications to Circuit Design (SMACD), 2017.

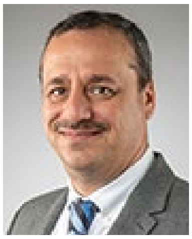

**Kais Abdulmawjood** (M'07) Kais Abdulmawjood is currently a Ph.D. student in Electrical Engineering, at University of Ontario Institute of Technology, Ontario, Canada. He received his MSc degree in Electric Engineering, Electronics and Communication, from Al-Mustansiriya University in 1998. His B.Sc. was in Electrical Engineering, from Baghdad University. He works as a Laboratory Manager in the Electrical and Computer Engineering Program, Texas A&M University at Qatar. Prior to joining Texas, A&M University at Qatar in 2007, Kais worked as head of the Computer Center at AlMustanisriya University. He also served as a scientific coordinator in the Computer and Software Engineering Department, Faculty of Engineering. While at AlMustansirya University, Kais served as an Adjunct Lecturer at Computer Science and Information Technology, University of Technology, Iraq, and as a Visiting Lecturer at Computer College, Thimar University, Yemen.

**Shady S. Refaat** received the B.A.Sc, M.Sc., and Ph.D. degrees in Electrical Engineering in 2002, 2007, and 2013, respectively, all from Cairo University, Giza, Egypt. He has worked in the industry for more than 12 years as Engineering Team Leader, Senior Electrical Engineer, and Electrical Design Engineer on various electrical engineering projects. Currently, he is an associate research scientist in the Department of Electrical and Computer Engineering, Texas A&M University at Qatar. He is a senior member of the Institute of Electrical and Electronics Engineers (IEEE), a member of The Institution of Engineering and Technology (IET), a member of the Smart Grid Center – Extension in Qatar (SGC-Q). He has published more than 115 journal and conference articles and one book. His principal work area focuses on electrical machines, power systems, smart grid, Big Data, energy management systems, reliability of power grids and electric machinery, fault detection, and condition monitoring and development of fault-tolerant systems. Also, he has participated and leads several scientific projects over the last eight years. He has successfully realized many potential research projects.

**Samer Alsadi** Received the MSc degree in Power Systems from Mendeleyev University of Chemical Technology of Russia, Moscow, in 1996 and the PhD degree in Electrical and Power Transmission Installation/Installer, General from Moscow Power Engineering Institute (Technical University). He worked as a Consultant in Jenin's municipality for one year, and he is currently an Associate Professor at the Electrical Engineering Department, Faculty of Engineering and Technology, Palestine Technical University-Kadoorie, Tulkarm, Palestine. He is a senior member of the Institute of Electrical and Electronics Engineers (IEEE). His research interests focus on mesh networking, network and systems, protection systems, forecasting and transmission planning.

**Walid G. Morsi** (S'07–M'09–SM'16) was born in Ismailia, Egypt, in 1975. He received the B.Sc. (Eng.) and M.Sc. (Eng.) degrees in electrical engineering from Suez Canal University, Ismailia, in 1998 and 2002, respectively, and the Ph.D. degree in electrical engineering from Dalhousie University, Halifax, NS, Canada, in 2009.

He was a Killam Memorial Predoctoral Scholar with Dalhousie University, and then he was an Assistant Professor with the Department of Electrical and Computer Engineering, University of New Brunswick, Fredericton, NB, Canada. He is currently a Professor with the Department of Electrical Computer and Software Engineering, Faculty of

Engineering and Applied Science, Ontario Tech University (UOIT), Oshawa, ON, Canada. His research interests include smart grid, power quality/disturbance data analytics, transportation electrification, energy monitoring, management, and automation of electric power systems.

Dr. Morsi is a registered Professional Engineer (P.Eng.) with the Association of Professional Engineers in Ontario (PEO).